Na+ is shifted from the extracellular to the intracellular compartment and is not inactivated by glycosaminoglycans during high salt conditions in rats

Irene Matre Thowsen[1], Tine V. Karlsen[1], Elham Nikpey[1,2] , Hanne Haslene-Hox[3], Trude Skogstrand[1], Gwendalyn J. Randolph[4], Bernd H. Zinselmeyer[4], Olav Tenstad[1] and Helge Wiig[1]

[1]*Department of Biomedicine, University of Bergen, Bergen, Norway*
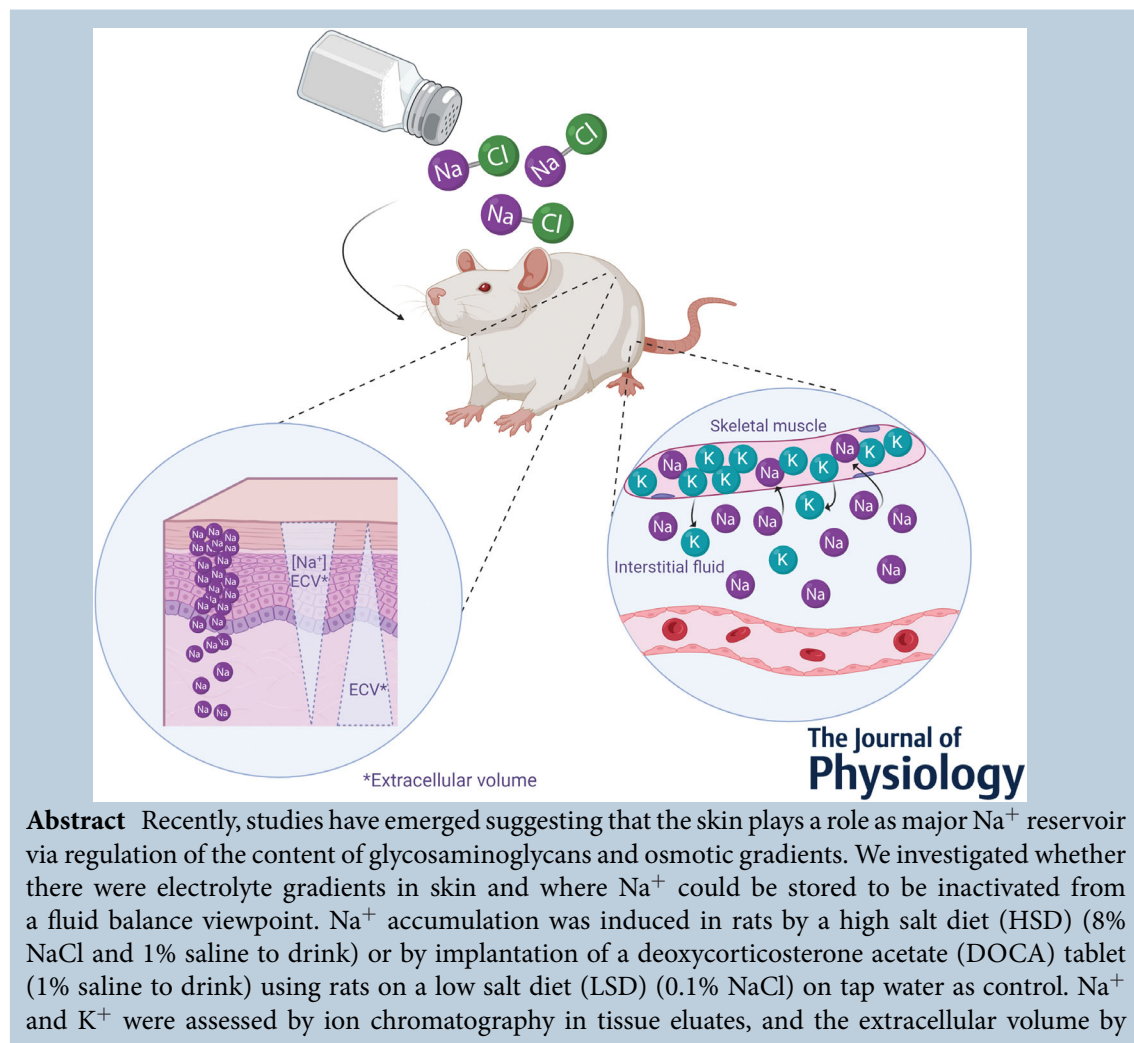[2]*Department of Medicine, Haukeland University Hospital, Bergen, Norway*
[3]*Department of Biotechnology and Nanomedicine, SINTEF Industry, Trondheim, Norway*
[4]*Department of Pathology & Immunology, Division of Immunobiology, Washington University, St Louis, MO, USA*

The Journal of Physiology

Abstract Recently, studies have emerged suggesting that the skin plays a role as major Na+ reservoir via regulation of the content of glycosaminoglycans and osmotic gradients. We investigated whether there were electrolyte gradients in skin and where Na+ could be stored to be inactivated from a fluid balance viewpoint. Na+ accumulation was induced in rats by a high salt diet (HSD) (8% NaCl and 1% saline to drink) or by implantation of a deoxycorticosterone acetate (DOCA) tablet (1% saline to drink) using rats on a low salt diet (LSD) (0.1% NaCl) on tap water as control. Na+ and K+ were assessed by ion chromatography in tissue eluates, and the extracellular volume by

equilibration of ^{51}Cr-EDTA. By tangential sectioning of the skin, we found a low Na$^+$ content and extracellular volume in epidermis, both parameters rising by $\sim$30% and 100%, respectively, in LSD and even more in HSD and DOCA when entering dermis. We found evidence for an extracellular Na$^+$ gradient from epidermis to dermis shown by an estimated concentration in epidermis $\sim$2 and 4–5 times that of dermis in HSD and DOCA-salt. There was intracellular storage of Na$^+$ in skin, muscle, and myocardium without a concomitant increase in hydration. Our data suggest that there is a hydration-dependent high interstitial fluid Na$^+$ concentration that will contribute to the skin barrier and thus be a mechanism for limiting water loss. Salt stress results in intracellular storage of Na$^+$ in exchange with K$^+$ in skeletal muscle and myocardium that may have electromechanical consequences.

Abstract figure legend Sprague–Dawley (SD) rats were given either high salt diet or deoxycorticosterone acetate (DOCA)-salt diet using SD rats on a low salt diet as a control. After 2 weeks on the diet, the rats were given the extracellular tracer ^{51}Cr-EDTA. Following 120 min of circulation time, the rats were killed, and shaved back skin was taken to the cryostat where tangential sections of epidermis, dermis, and subcutis were made to determine extracellular volume (ECV) and Na$^+$ concentration. There was a Na$^+$ gradient in ECV shown by a higher Na$^+$ concentration in the superficial layers of the skin compared to deeper layers. Analysis of skeletal muscle interstitial fluid and tissue showed that high salt conditions resulted in an increase in intracellular Na$^+$ that was exchanged with K$^+$.

Key points

- Studies have suggested that Na$^+$ can be retained or removed without commensurate water retention or loss, and that the skin plays a role as major Na$^+$ reservoir via regulation of the content of glycosaminoglycans and osmotic gradients.
- In the present study, we investigated whether there were electrolyte gradients in skin and where Na$^+$ could be stored to be inactivated from a fluid balance viewpoint.
- We used two common models for salt-sensitive hypertension: high salt and a deoxycorticosterone salt diet.
- We found a hydration-dependent high interstitial fluid Na$^+$ concentration that will contribute to the skin barrier and thus be a mechanism for limiting water loss.
- There was intracellular Na$^+$ storage in muscle and myocardium without a concomitant increase in hydration, comprising storage that may have electromechanical consequences in salt stress.

Introduction

It is textbook knowledge that body fluid volume and thereby body Na$^+$ content must be maintained within narrow limits to maintain blood pressure homeostasis (Guyton et al., 1974). During recent years, however, several long-term studies in humans have shown that Na$^+$ can be retained or removed from the subjects' bodies without commensurate water retention or loss (Heer et al., 2000; Palacios et al., 2004; Rakova et al., 2013; Titze et al., 2002), suggesting that Na$^+$ could be stored

Irene Matre Thowsen is an MD specialised in medical oncology. She is currently carrying out her PhD work in the Cardiovascular Research Group at Department of Biomedicine at the University of Bergen under supervision of Professor Helge Wiig, Associate Professor Tine V. Karlsen and Dr Anne-Maj Samuelsson. The working title of the thesis is 'New actors in blood pressure regulation. The extracellular microenvironment, lymphatics, and VEGF-B'. The PhD fellowship was funded by the Norwegian Health Association.

somewhere in the body and thereby be 'inactive' from a fluid balance viewpoint (Titze et al., 2003). Such storage would require 'new' extrarenal, tissue-specific regulatory mechanisms that control the release and storage of Na$^+$ from a kidney independent reservoir. Studies have suggested that the skin interstitium, with its high content of glycosaminoglycans (GAGs), plays a major role as Na$^+$ reservoir (Machnik et al., 2009; Schafflhuber et al., 2007; Titze et al., 2006), again implicating that there is not a strict isotonicity of all body fluids and that skin and plasma electrolyte concentrations do not necessarily equilibrate. This observation might have been part of the explanation for our finding that rats on a high salt diet (HSD) resulting in Na$^+$ accumulation in skin have a tissue that is hyperosmotic relative to plasma (Wiig et al., 2013). Even though the skin was hyperosmotic, we found no osmotic gradient between plasma and lymph assumed equal to interstitial fluid in salt accumulation induced by HSD and deoxycorticosterone acetate (DOCA)-salt (Nikpey et al., 2017). We could, however, not exclude that there were local gradients in major osmolytes between the most superficial layer next to the keratinocytes and the deeper dermis, which would have supported a hypothesis a functional counter-current system in the skin (Hofmeister et al., 2015) enabling differential control of its own microenvironment. Although quantitatively not so important, our finding of an increased epidermal to dermal osmolyte gradient for urea in rat skin that was increased in salt accumulation supports differential microenvironmental control. Surprisingly, a lower content of Na$^+$ in epidermis-dermis than in the deeper dermis indicated that Na$^+$ does not contribute to this gradient (Nikpey et al., 2017). As we pointed out, however, Na$^+$ will predominantly distribute in the extracellular space, resulting in a higher concentration in its available space in the more cell rich epidermis than in dermis, and may thereby contribute to the osmotic gradient *in vivo*.

Although the electrolyte content has been measured across epidermis with electron probe analysis in human (Warner et al., 1988), as well as guinea-pig skin (Wei et al., 1982), these studies could not account for the electrolyte distribution volume. Because of its potential functional importance, we decided to test the hypothesis that there is a gradient in Na$^+$ in skin such that there is an increasing concentration closer to the surface, with this gradient being a consequence of a counter-current effect resembling the one used for electrolyte gradient formation in the kidney medulla.

Methods

Ethics statement

All animal experiments were conducted in accordance with the regulations of the Norwegian State Commission for Laboratory Animals, which are consistent with the European Convention for the Protection of Vertebrate Animals used for Experiments and Other Scientific Purpose. Experiments were performed with the approval from the Association for Assessment and Accreditation of Laboratory Animal Care (AAALAC) International accredited Animal Care and Use Program at the University of Bergen and the Norwegian Food and Safety Authority (licenses FOTS ID 10508 and 26248).

Animal protocols

The experiments were performed in male Sprague–Dawley rats ($n = 96$), 11–15 weeks old with a body weight of 350–450 g. The animals were housed in a humidity and temperature-controlled environment under a 12:12 h light/dark photocycle. Anaesthesia was induced with 3% and maintained with 1.5–2% isoflurane (IsoFlo®Vet 100%; Abbott Laboratories Ltd, Sittingbourne, UK) in 100% O$_2$. This procedure was used during both acute terminal experiments and during DOCA-tablet implantation (see below). Under isoflurane anaesthesia, the animals were kept on a heating pad supplemented with a heating lamp when necessary, and their body temperature was monitored and maintained at 37–38°C.

The rats were randomly assigned to either a low salt diet (LSD) with <0.1% NaCl in the chow and tap water to drink ($n = 41$), HSD with 8% NaCl in the chow and 1% saline to drink ($n = 31$) or DOCA-salt, where a 50 mg week^{-1} prolonged-release DOCA pellet (150 mg; Innovative Research of America, Sarasota, FL, USA) was implanted s.c. in the neck region and the rats given 1% saline to drink ($n = 24$). The animals were killed at the end of experiment under deep isoflurane anaesthesia by a terminal cardiac blood sample before excision of the heart, except for the multiphoton experiments, where cardiac arrest was induced by an i.v. injection of saturated KCl.

The blood samples were left in room temperature for 30 min before being centrifuged at 2000 ***g*** for 10 min. Immediately after death of the rats, tissue samples were harvested and either prepared for ion chromatography by weighing and then drying the samples (see below) or stored at −20°C until further analysis. Skin for multiphoton microscopy was fixed in 4% paraformaldehyde for 3 days before further processing.

Ion chromatography analyses

All samples to be analysed by ion chromatography were weighed directly after harvesting to determine the wet weight of the sample and then dried in a heating chamber at 50°C until a stable weight was attained. The dried tissue samples were eluted in ultrapure water (MilliQ; Millipore Corp., Burlington, MA, USA) for 1 week for equilibration.

Samples from skin, skeletal muscle, apex of the heart, and 40 μL of serum were eluted in 5 mL of ultrapure water. The tangential skin sections (see below) were eluted in 500 μL of ultrapure water. During elution, the samples were placed on a platform rocker in a cold room at 4°C.

Na$^+$ and K$^+$ in the eluted tissue solutions were baseline separated in a 10 min 7.5–60 mmol/LMSA gradient at a flow rate of 0.2 mL min^{-1} by a Dionex IonPac CS 16-4 μm RFIC analytical column (2 × 250 mm, P/N 088582) and guard (2 × 50 mm P/N 088583) using a Dionex Integrion HPLC System equipped with a CDRS 600 (2 mm) Cation Electrolytic Suppressor and a high pressure EGC 500 methane sulphonic acid eluent generator cartridge (Thermo Fisher Scientific, Waltham, MA, USA). Thereafter, ion content was related to tissue wet weight, dry weight, and water content.

In a separate series of experiments, we assessed whether Na$^+$ and K$^+$ are released to the solvent and not bound to tissue elements by digesting the skin in nitric acid. Following weighing, the samples were eluted for 1 week in 50 mL of ultrapure water when placed on a platform rocker at 4°C. The samples were then removed, and the eluates analysed in the ion chromatograph. The samples were reweighed before being dried in a heating chamber at 50°C until a stable weight was attained, and dissolved in 200 μL of nitric acid (Nitric acid ROTIPURAN®Supra 69%; Carl Roth, Karlsruhe, Germany) for 1−2 h in a heating chamber at 70°C. When the tissue was completely dissolved and the solution was clear, 120 μL of hydrogen peroxide and 20 mL of ultrapure H$_2$O was added and mixed well. Thereafter, 100 μL of this solution was diluted further in 100 μL of ultrapure water and analysed in the ion chromatograph.

Tangential sectioning of skin

Frozen sections of skin were stained by haematoxylin and eosin in accordance with the standard protocol. The thickness of the different layers of the skin was measured, including the whole skin from the outer part of epidermis to muscle based on the morphological hallmarks, comprising epidermis stretches from stratum corneum to the basal layer, as well as dermis from the basal layer to the loose connective tissue and adipose tissue in the hypodermis. A minimum of four repeated measurements were carried out for each layer and averaged.

Shaved back skin was harvested directly after the animals were killed. Sequential tangential sections of epidermis (40 μm) and dermis and subcutis (100 μm) were made in a cryostat taking care to avoid evaporation. After being weighed and counted in the gamma counter (see below), the samples were placed in a heating chamber at 50°C until a stable weight was attained. Thereafter, the

samples were eluted in 500 μL of ultrapure water (MilliQ). The eluate was analysed in the ion chromatograph to determine ion content as described above.

Measurements of extracellular volume

Measurement of extracellular volume was performed in two separate series, where HSD ($n = 7$) was compared with LSD ($n = 7$), and DOCA-salt ($n = 8$) was compared with another LSD ($n = 8$) group. Two weeks into the diet regimen, the rats were anaesthetised with isoflurane and a catheter placed in the jugular vein for i.v. injection of extracellular tracer. Both kidney pedicles were ligated to prevent escape of tracer and fluid through the kidneys during the experiment. After i.v. injection, the ^{51}Cr-EDTA tracer (0.25 MBq in 0.15 mL of saline; PerkinElmer, Groningen, The Netherlands) was allowed 120 min of circulation time to ensure uniform distribution in the extracellular space before drawing a terminal cardiac blood sample and killing the rat by excising the heart. Directly thereafter, we harvested shaved full back skin for tangential skin sectioning (see above), hindlimb skeletal muscle, and heart. The samples were weighed and counted in a gamma counter (Packard-Cobra II Auto-Gamma; Perkin Elmer, Waltham, MA, USA). Extracellular volume was considered as the plasma equivalent space of ^{51}Cr-EDTA [i.e. (cpm/g tissue)/(cpm/mL plasma)].

Isolation of interstitial fluid from muscle

Rats were assigned to LSD ($n = 6$), HSD ($n = 6$), and DOCA-salt ($n = 7$) 2 weeks prior to implantation of nylon wicks in the muscle interstitium. Under isoflurane anaesthesia, multifilamentous nylon wicks, prewashed in acetone, ethanol, and distilled water, were implanted in the muscle interstitium as described in detail previously (Wiig et al., 1991). Briefly, the wicks were soaked in isotonic saline before implantation and were threaded into an 8–10 cm long PE-160 catheter. Wick implantation was through a small cut in the skin and muscle fascia at two locations in each hind limb, laterally along the gastrocnemius muscle, and medially along the gracilis muscle. After placing the catheter, the wick was pushed out with a PE-50 catheter. The skin incision was closed with a forceps and the wicks were left in for 90 min before being removed in a humidity chamber to avoid evaporation, prior to killing the animals. The wick ends and any bloodstained parts were cut off, and the wick transferred to a pre-weighed vial for reweighing and elution. The amount of interstitial fluid was calculated, and the eluate was analysed in the ion chromatograph. In this series, samples of serum, skin, muscle, and heart were also harvested for ion content analyses in the ion chromatograph.

Sulphated glycosaminoglycans

The amount of sulphated glycosaminoglycans (sGAG) was measured by a quantitative dye-binding method in two separate series. Freeze-dried skin samples were digested as described in detail previously by Sagstad et al. (2015), before the concentration of sGAGs was measured using the Blyscan sGAG assay kit (BC-B1000 or B-1000; Biocolor, Carrickfergus, UK) in accordance with the manufacturer's instructions. The procedure is based on 1.9-dimethylmethylene blue that provides a specific binding of the sulphated polysaccharide component of proteoglycans or the protein free sulphated glycosaminoglycan chains. Before analysis, the skin samples were defatted using a chloroform and methanol mixture (400 μL of chloroform and 200 μL of methanol), left in a gentle shaker for 24 h, then 150 μL of chloroform and 150 μL of ultrapure water were added for 2−4 h, followed by drying until a stable weight was attained before being used in the assay. The absorbance values at a wavelength of 650 nm were calculated using the SPECTRAmax® Spectrophotometer and SoftMax Pro (Molecular Devices, San Jose, CA, USA).

Collagen

The same method as for sGAGs was used for obtaining defatted dry weight in skin samples in the collagen assay. Collagen was measured by the Sircol$^{\text{TM}}$ Insoluble Collagen Assay (Biocolor) in accordance with the manufacturer's instructions using a SPECTRAmax® Spectrophotometer and SoftMax Pro to calculate absorbance values at a wavelength 550 nm. In another series, collagen was measured in LSD and HSD rats using a method based on the determination of hydroxyproline content as described by Sagstad et al. (2015) assuming a conversion factor of 6.94 μg of hydroxyproline per 1 mg of collagen as originally performed by Woessner (1961).

Hyaluronic acid

Hyaluronic acid (HA) in digested skin samples (see above) was determined using a hyaluronic acid test kit (Catalog number 029-001; Corgenix, Broomsfield, CO, USA) in accordance with the manufacturer's instructions.

Multiphoton microscopy

Under isoflurane anaesthesia, a catheter was inserted into the jugular vein and secured. Subsequently, 300 μL of Lycopersicon Esculentum (Tomato) Lectin (LEL, TL), DyLight® 649 (DL-1178-1) (Vector Labs, Burlingame, CA, USA) was injected i.v. and allowed a circulation time of ∼7 min. After killing the rat, hair was removed by hair removal cream, and skin samples were harvested from paw, back, thigh, and tail and fixed flat on a Sylgard plate in 4% paraformaldehyde for 3 days. Then, the skin was dehydrated by incubating in increasing ethanol/PBS concentrations (30%, 50%, 70%, 90%, and two times 100% for 12 h each.)

For refractory index matching, the tissue was transferred to a customised aluminium chamber in methyl salicylate. A second chamber with a large glass cover-slide bottom was placed on the tissue and air bubbles were removed. The second chamber was filled to a height of 2 mm with water to use the 25 × 0.95 NA WD 2.5 mm water dipping objective of our customised 2P microscope (Leica Microsystems, Wetzlar, Germany).

Images were collected using a customised Leica SP8 two-photon microscope (Leica Microsystems) equipped with a 25 × 0.95 NA WD 2.5 mm water immersion objective, and two femtosecond-pulsing tunable Ti:Sapphir lasers (Mai Tai HP DeepSee and InSight DS+), both from Spectra-Physics (Mountain View, CA, USA). The sample was excited at 820 nm and the fluorescence emission was guided directly to four external detectors in dendritic arrangement (two hybrid and two classical photomultiplier tubes). For signal separation, three dichroic beam splitters (458, 505, and 605 nm; Semrock, Rochester, NY, USA) were used. The SHG (second-harmonic generation) was collected below 458 nm, autofluorescence was collected between 505 and 605 nm, and the emission of DyLight® 649 was collected between 605 nm and 700 nm. Images were processed and rendered with Imaris cell imaging software (Oxford Instruments, Abingdon, UK).

Statistical analysis

Statistical analyses and graphs were constructed using PRISM, version 8.0 (GraphPad Software Inc., San Diego, CA, USA). Outliers identified by ROUT with $Q = 1\%$ were excluded. Normality was tested by the D'Agostino & Pearson test when $n \geq 8$. When $n < 8$, a Shapiro–Wilk test was used. ANOVA or mixed-effects analyses followed by Sidak's multiple comparisons test was used when assessing three or more groups. Unpaired Student's t tests were used when comparing two groups. Values are given as the mean ± SD. $P < 0.05$ was considered statistically significant.

Results

Tissue electrolyte concentration measured by ion chromatography

We first assessed Na$^+$ and K$^+$ content with ion chromatography after elution in ultrapure water in whole back skin, as well as after separation in dermis

and subcutis by blunt dissection (Reed et al., 1989). As shown in Fig. 1*A*, there was a significant accumulation of Na^+ expressed on a dry weight (DW) basis in both HSD ($n = 6$) (mean ± SD) (Na^+ 203.6 ± 13.0 mmol kg^{-1} DW, $P = 0.0004$) and DOCA-salt ($n = 7$) (Na^+ 206.7 ± 18.0 mmol kg^{-1} DW, $P = 0.0002$) compared to LSD ($n = 6$) (Na^+ 156.1 ± 17.9 mmol kg^{-1} DW) in whole skin. Moreover, the skin water content was slightly increased in HSD, but not DOCA-salt, compared to LSD. Na^+ related to water content also increased, in both HSD and DOCA-salt, compared to LSD. In

dermis, there was an increase in Na^+ in HSD ($n = 6$) (Na^+ 198.2 ± 9.3 mmol kg^{-1} DW, $P = 0.0002$) and DOCA-salt ($n = 7$) (Na^+ 192.6 ± 12.8 mmol kg^{-1} DW, $P = 0.0004$) compared to LSD ($n = 3$) (Na^+ 145.7 ± 5.8) (Fig. 1*B*). Interestingly, ($Na^+ + K^+$) increased from ~140 in LSD to ~160 mmol L^{-1} H_2O in dermis in HSD and DOCA-salt (Fig. 1*B*), a difference that was not detected when analysing total skin, thus showing electrolyte accumulation in the dermal layer.

Serum concentrations of Na^+ both in HSD ($n = 5$) (Na^+ 146.8 ± 3.2 mmol L^{-1}) and DOCA-salt ($n = 7$) (Na^+
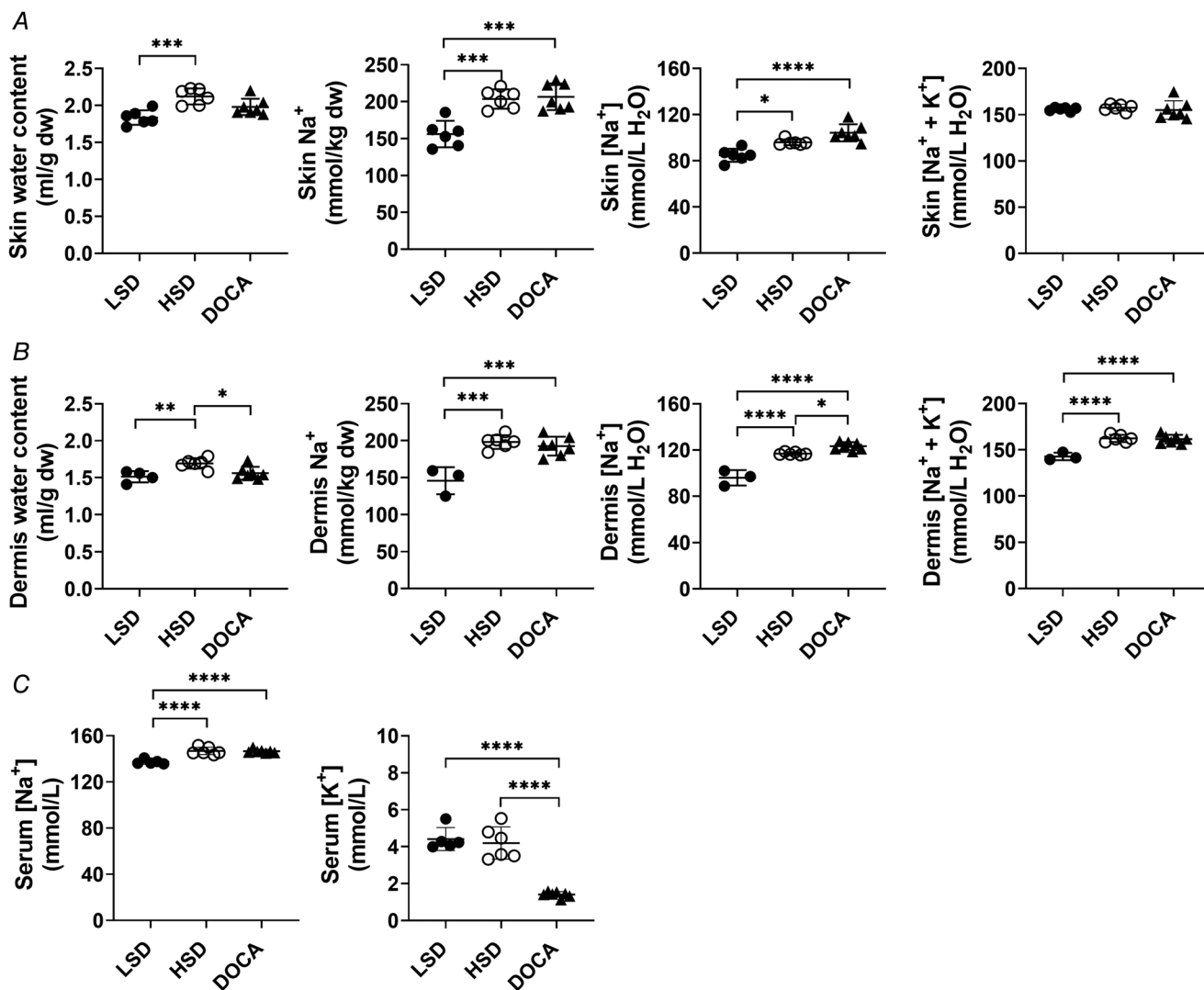

Figure 1. Na^+ and K^+ content in whole skin and dermis, and concentrations in serum
Individual values of water content related to dry weight (DW), Na^+ related to dry weight (DW) and water, $Na^+ + K^+$ related to water in whole skin (LSD, $n = 6$; HSD, $n = 6$; DOCA, $n = 7$) (*A*) and dermis [LSD, $n = 3$ (except for water content LSD, $n = 4$); HSD, $n = 6$; DOCA, $n = 7$] (*B*), individual values of Na^+ and K^+ in serum (LSD, $n = 5$; HSD, $n = 6$; DOCA, $n = 7$) (*C*), all isolated from rats after a low salt diet (LSD) (●), high salt diet (HSD) (○), and deoxycorticosterone (DOCA)-salt diet (DOCA) (▲). Also shown are the mean ± SD. In serum, there was a significant increase in Na^+ in rats on HSD and DOCA-salt diet, as well as a significant corresponding decrease of Na^+ in the DOCA-salt diet group. *$P < 0.05$, **$P < 0.01$, ***$P < 0.001$, ****$P < 0.0001$ compared to ANOVA followed by Sidak's multiple comparisons test.

146.6 ± 1.6 mmol L^{-1}) increased ($P < 0.0001$) compared to LSD ($n = 5$) (Na$^+$ 137.4 ± 2.1 mmol L^{-1}) (Fig. 1*C*), with a corresponding decrease ($P < 0.0001$) in potassium in DOCA-salt ($n = 7$) (K$^+$ 1.4 ± 0.2 mmol L^{-1}) compared to LSD ($n = 5$) (K$^+$ 4.4 ± 0.6 mmol L^{-1}).

We next tested whether Na$^+$ and K$^+$ were bound to tissue elements by comparing Na$^+$ and K$^+$ in whole skin after elution in ultrapure water with the values from the same skin sample following complete digestion of tissue elements in nitric acid. Compared to background signal, we found that no Na$^+$ and K$^+$ remained in skin in LSD and HSD conditions. Thus, the Na$^+$ content following digestion was −0.3 ± 0.8% ($n = 10$) and −0.3 ± 0.6% ($n = 5$) of the content after elution in skin from LSD and HSD rats, respectively. Similar numbers were found for K$^+$. The cation binding to the extracellular matrix was thus negligible.

Extracellular matrix components in high salt conditions

We assessed the components of the extracellular matrix, that is, collagen and GAGs. GAGs consist of hyaluronan and sulphated GAGs (sGAGs), the latter being proposed to play a role in salt storage (Schafflhuber et al., 2007; Titze et al., 2004).

In whole skin, sGAGs averaged (mean ± SD) 7.0 ± 1.5 mg per g fat free dry weight (DW) in LSD ($n = 14$), with a corresponding value for HSD ($n = 10$) of 7.5 ± 0.9 mg g^{-1} ($P = 0.975$). Interestingly, after DOCA-salt ($n = 6$), we found a mean sGAG concentration of 4.9 ± 0.4 mg g^{-1} DW, which was significantly lower than the corresponding concentration in LSD ($P = 0.0031$) and HSD ($P = 0.0004$) conditions (Fig. 2*A*). A similar pattern and similar numbers were found for sGAGs in dermis: LSD 6.7 ± 1.2 mg g^{-1} DW ($n = 15$), HSD 6.7 ± 1.5 mg g^{-1} DW ($n = 10$), and DOCA-salt 4.9 ± 0.4 mg g^{-1} DW ($n = 6$), with the latter value lower than LSD ($P = 0.0238$), as well as HSD ($P = 0.0349$) (Fig. 2*A*). There was no difference in sGAGs between the groups in subcutis: LSD 5.8 ± 1.4, HSD 6.0 ± 0.7, and DOCA-salt 4.9 ± 0.9 mg g^{-1} DW) (Fig. 2*A*).

We also determined hyaluronan, another major GAG component in LSD ($n = 10$) and HSD ($n = 10$) rats and found no effect of the diet. Thus, whole skin LSD had a mean content of HA of 0.65 ± 0.27 mg g^{-1} fat free DW in LSD and 0.79 ± 0.37 mg g^{-1} DW in HSD ($P = 0.8529$). In dermis, the respective numbers were 1.03 ± 0.17 mg g^{-1} DW and 1.06 ± 0.33 mg g^{-1} DW ($P = 0.9991$), whereas, in subcutis, HA averaged 1.55 ± 0.61 and 1.60 ± 0.57 mg g^{-1} DW, in LSD and HSD ($P = 0.9919$), respectively (Fig. 2*B*). Interestingly, the reduced sGAG in the DOCA-salt group implies that the degree of GAG sulphation was reduced in

the DOCA-salt group that retained most salt and thus that the capacity for 'inactive' Na$^+$ storage was reduced.

Next, we analysed collagen, the major structural component of the interstitium. In whole skin, the mean collagen content per fat free dry weight was 0.51 ± 0.05, 0.58 ± 0.01, and 0.60 ± 0.07 mg mg^{-1} fat free DW for LSD ($n = 5$), HSD ($n = 5$, $P = 0.5724$), and DOCA-salt ($n = 6$, $P = 0.2407$), respectively (Fig. 2*C*). The corresponding
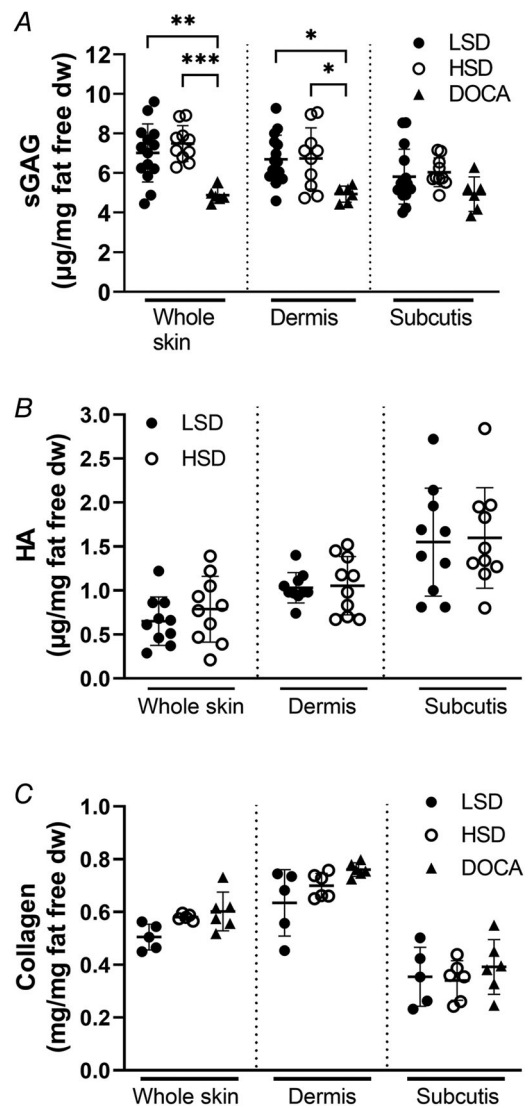

Figure 2. Extracellular matrix components in high salt conditions
A, individual values for sulphated GAGs (sGAGs) in whole skin, dermis, and subcutis in low salt diet (LSD) ($n = 14$) (●), high salt diet (HSD) ($n = 10$) (○), and deoxycorticosterone (DOCA)-salt diet (DOCA) ($n = 6$) (▲). Also shown are the mean ± SD. *$P < 0.05$, **$P < 0.01$, ***$P < 0.001$ compared to ANOVA followed by Sidak's multiple comparisons test. *B*, individual values for hyaluronan (HA) in whole skin, dermis and subcutis LSD ($n = 10$) (●) and HSD ($n = 10$) (○). *C*, individual values for collagen in whole skin, dermis and subcutis in LSD ($n = 5$) (●), HSD ($n = 6$) (○), and DOCA-salt diet ($n = 6$) (▲).

numbers for dermis were 0.63 ± 0.13, 0.70 ± 0.05, and 0.76 ± 0.03 mg mg^{-1} fat free DW, and, in subcutis, 0.35 ± 0.11, 0.34 ± 0.08, and 0.39 ± 0.10 mg mg^{-1} fat free DW (Fig. 2*C*).

Thickness of skin assessed by histology

We then measured the thickness of epidermis, dermis and subcutis in back skin from LSD, HSD, and DOCA-salt treated rats that was needed to determine thickness of tangential sections. High salt diets resulted in a reduction in whole skin, as well as epidermis and dermis, a reduction in thickness that was statistically significant for DOCA-salt only. The thickness of whole skin averaged (mean ± SD) 897 ± 149 μm (*n* = 9) in LSD and 497 ± 62 μm (*n* = 5) in DOCA-salt (*P* = 0.0001). The respective numbers for epidermis were 43 ± 8 μm (LSD) (*n* = 9) and 30 ± 8 μm (DOCA-salt) (*n* = 4) (*P* = 0.020). The respective numbers for epidermis were 43 ± 8 μm (LSD) (*n* = 9) and 30 ± 8 μm (DOCA-salt) (*n* = 4) (*P* < 0.05).

Electrolyte and extracellular volume gradients in skin

To investigate whether there were gradients in Na$^+$ and K$^+$ from the surface to deeper layers of the , we made tangential (i.e. horizontal) sections of frozen tissue in a cryostat and eluted samples followed by ion chromatography for electrolyte determination. Because of technical challenges related to sectioning, we used 40 μm sections for LSD, HSD, and DOCA-salt even if the epidermis in the latter was thinner than this.

The analysis of Na$^+$ and K$^+$ in different skin depths was performed in two separate series of animals. First, LSD was compared to HSD, and, as shown in Fig. 3*A*, the curves for water content were not different for these two groups. If, however, we normalise the hydration at various depths to that of epidermis there was a significant difference between the diet regimens. Thus, hydration in deeper layers in HSD increased by 42−105%, with a corresponding range for LSD of 16−37% (*P* = 0.044, two-way ANOVA; mixed effects model). Na$^+$ relative to dry weight in HSD was about twice that of LSD in deeper layers of dermis reflecting different Na$^+$ storage dependent on diet regimen. When comparing Na$^+$ and (Na$^+$+K$^+$) related to water content in the samples, however, the corresponding data points for two groups were not different. It should be noted that the mean Na$^+$ concentration over water was higher in HSD than in LSD except for one skin depth, thus reflecting the overall shape of the Na$^+$ relative to dry weight curve.

Because it has been proposed that Na$^+$ is up-concentrated in the superficial part of the skin (Hofmeister et al., 2015), we focused on the trans-ition zone between epidermis and dermis. By contrast to what has been proposed, there was a tendency to a lower mean Na$^+$ content in epidermis (mean ± SD) (100.4 ± 21.3 mmol kg^{-1} DW) than in dermis at 40−140 μm depth (128.9 ± 20.0 mmol kg^{-1} DW) in LSD (*n* = 7) (*P* = 0.1052), whereas, in HSD (*n* = 6), a significantly lower mean Na$^+$ was found in epidermis compared to superficial dermis (97.5 ± 25.1 and 160.4 ± 24.0 mmol kg^{-1} DW, respectively) (*P* = 0.0003) (Fig. 3*C*). As for HSD, the Na$^+$ content was also higher in some layers of dermis when comparing DOCA-salt with the LSD group (Fig. 3*B*), and this applies to both Na$^+$ related to dry weight and to water content. (Na$^+$+K$^+$) curves for this series were overlapping, with exception of one point in in the deepest layer of dermis. When considering water content in this second series of experiments, it became apparent that both LSD and DOCA-salt groups had a much lower water content in epidermis than the first LSD and HSD series, although values were similar in dermis in the two series. As for the first series, there was no evidence of selective up-concentration in epidermis in this second series, Na$^+$ in first layer of dermis at 40−140 μm was significantly higher than in epidermis, in both LSD (*n* = 8) (149.1 ± 14.5 and 74.0 ± 21.2 mmol kg^{-1} DW) and DOCA-salt groups (*n* = 8) (159.0 ± 20.3 and 65.6 ± 10.8 mmol kg^{-1} DW (*P* < 0.0001) (Fig. 3*C*). Notably, for both series, there was no selective accumulation of Na$^+$ in superficial dermis that tended to have a lower Na$^+$ concentration than deeper dermis.

Because the concentrations of Na$^+$ and K$^+$ are different in the extracellular and intracellular fluid phase, we next determined these fluid spaces in tangential sections of skin following equilibration of the extracellular tracer ^{51}Cr-EDTA in two separate series. In the first series, HSD was compared to LSD, and although the extracellular volume (ECV) pattern across the skin was similar, there was a tendency to a higher ECV in HSD compared to LSD (Fig. 4*A*), with similar results when comparing DOCA-salt with LSD (Fig. 4*B*). Although not different between diet regimens, there was apparently a substantial increase in ECV from epidermis to the most superficial layer of dermis for all groups reflecting a higher cell content in the former layer. Thus, mean ECV was 0.19 ± 0.04 and 0.21 ± 0.07 mL g^{-1} wet weight (WW) in LSD (*n* = 7) and HSD (*n* = 5) in epidermis, increasing to 0.43 ± 0.05 and 0.46 ± 0.04 mL g^{-1} WW, respectively, in the first layer of dermis at 40−140 μm depth (*P* < 0.0001) (Fig. 4*A*). Similar corresponding volumes and pattern were found in the second series, although these rats in both groups overall had a lower water content in epidermis compared to the first series, which affects both ECV and ICV. Thus, in DOCA-salt (*n* = 8) rats, the mean ECV was 0.08 ± 0.03 mL g^{-1} WW in epidermis, increasing to 0.47 ± 0.05 mL g^{-1} WW in superficial

dermis ($P < 0.0001$), with corresponding numbers in LSD ($n = 7$) of 0.11 ± 0.04 and 0.49 ± 0.03 mL g^{-1} WW ($P < 0.0001$) (Fig. 4*B*).

Na$^+$ and K$^+$ relative to ECV at different skin depths. We estimated extracellular fluid Na$^+$ concentration by assigning the measured Na$^+$ to ECV after subtraction of an intracellular fraction having a concentration of 10 mM (Hall, 2016). Such calculations suggested there was a Na$^+$ gradient in ECV from epidermis to dermis in HSD and DOCA-salt and in one of the LSD groups (Fig. 4, middle columns). When focusing on the epidermal–dermal junction, the estimated ECV concentration in epidermis was ∼2 and 4−5 times

that of dermis in HSD and DOCA-salt, respectively (Fig. 4, right columns). Surprisingly, there was also a Na$^+$ gradient with a magnitude similar to that in DOCA-salt in the corresponding LSD group (Fig. 4, right columns).

Vessel structure in skin

Our assessment of extracellular fluid in skin indicated that the Na$^+$ concentration is higher in epidermis. Next, we therefore studied the structure of skin vasculature asking whether there could be an anatomical correlate to this observation as suggested by others (Hofmeister et al., 2015).
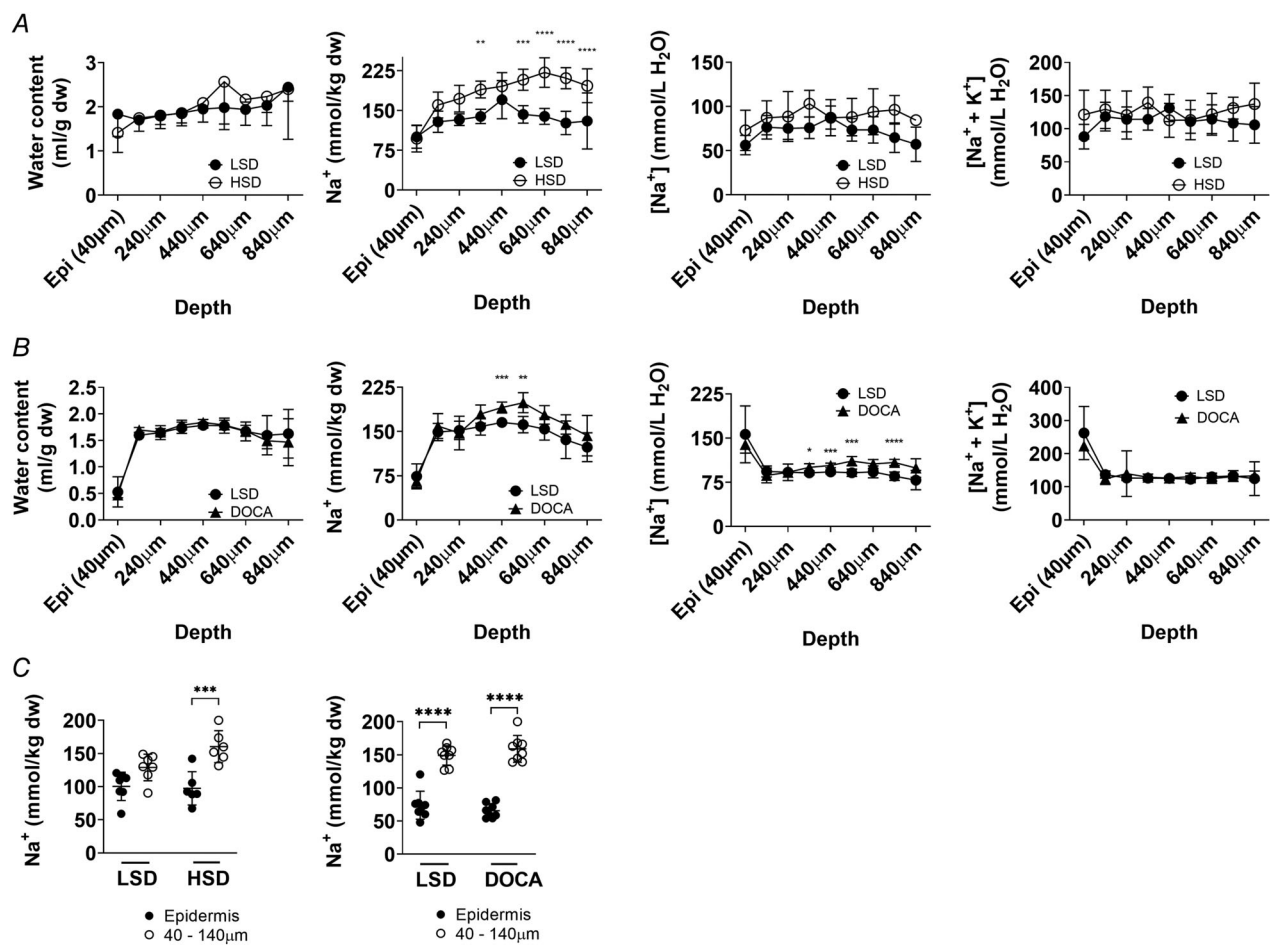

Figure 3. Water content, Na$^+$ related to dry weight and water, and Na$^+$+K$^+$ related to water at different depths in skin
Water content per dry weight (DW) of sample, Na$^+$ related to dry weight, Na$^+$ related to water in sample and Na$^+$+K$^+$ related to water in sample of each layer of the skin at different skin depths in low salt diet (LSD) ($n = 7$) (●) and high salt diet (HSD) ($n = 6$) (○) series (*A*) and in LSD ($n = 8$) (●), and deoxycorticosterone (DOCA)-salt diet (DOCA) ($n = 8$) (▲) series (*B*). Values are the mean $\pm$ SD except for (*A*) hydration showing 1 SD. *$P < 0.05$, **$P < 0.01$, ***$P < 0.001$, ****$P < 0.0001$, compared to mixed-effects analysis followed by Sidak's multiple comparisons test. Dotted lines demarcate the transition from epidermis to dermis. *C*, individual values and the mean $\pm$ SD of Na$^+$ related to dry weight in epidermis (●) compared to superficial layer of dermis from 40 to 140 μm (○) for LSD compared to HSD and LSD compared to DOCA-salt diet (ANOVA followed by Sidak's multiple comparisons test. *$P < 0.05$, ****$P < 0.0001$).

Two-photon microscopy of back skin is shown in Fig. 5. We were able to image from the epidermal surface into deeper dermis. Skin vessels were rather disorganised with an extensive capillary network that appeared to extend to underneath the epidermis (green auto-fluorescence region). The vessels of variable dimension appeared to be parallel to the surface. Notably, we found no indications of vessel loops extending perpendicularly from vessels going parallel to the surface up to epidermis, except for minor loops around some of the adipocytes (online video). A similar structure was found in paw skin.

Na$^+$ is stored in skeletal and cardiac muscle during high salt conditions

In skeletal muscle, HSD did not affect ECV, but there was a modest increase in ECV in the DOCA-salt group

(Fig. 6A). There was, however, a significant increase in Na$^+$ compared to LSD in both HSD and DOCA-salt relative to dry weight, as well as water content, most prominent in the latter (Fig. 6A). Interestingly, (Na$^+$+K$^+$) relative to water was not different with averages in the range of 150−160 mmol L^{-1} H$_2$O (Fig. 6A). This observation implies that there was a shift of Na$^+$ from the extra- to the intracellular compartment with a transfer of K$^+$ in the opposite direction. A reduced K$^+$ might be expected because of DOCA-salt treatment resulting in hypokalaemia, but that such reduction in K$^+$ concentration also occurred in HSD suggests that Na$^+$/K$^+$ shifts in skeletal muscle might be a general feature during salt loading. Findings in the cardiac muscle paralleled the results from the skeletal muscle, comprising an increased ECV in DOCA-salt, an increase in Na$^+$ relative to dry weight and water, most pronounced for DOCA-salt, and
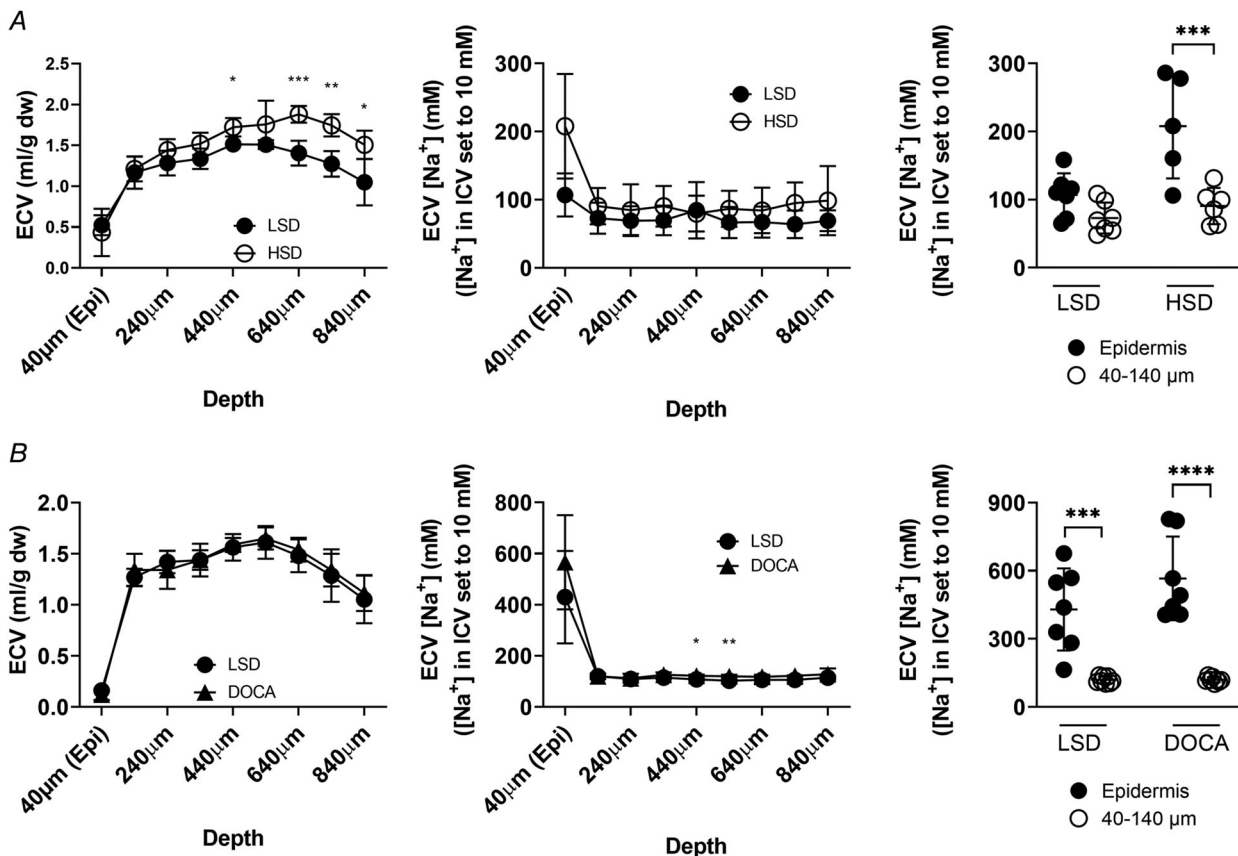

Figure 4. ECV and Na$^+$ related to ECV at different skin depths
Extracellular fluid volume (ECV) and Na$^+$ related to ECV assuming 10 mM Na$^+$ being intracellular, in high salt diet (HSD) (*n* = 6) (○) and low salt diet (LSD) (*n* = 7) (●) (*A*), and deoxycorticosterone (DOCA)-salt diet (DOCA) (*n* = 8) (▲) and LSD (*n* = 8) (●) (*B*). In both series, the curves are overlapping, with a tendency to a higher ECV in HSD than in LSD, being statistically significant at 640 μm depth only (*P* < 0.05). In DOCA-salt diet, Na$^+$ related to ECV was significantly higher at two points in dermis compared to LSD (*P* < 0.05), using mixed-effects analysis followed by Sidak's multiple comparisons test. Values are the mean ± SD. **P* < 0.05, ***P* < 0.01. Individual values and the mean ± SD of Na$^+$ related to ECV in epidermis (●) compared to superficial layer of dermis at 40−140 μm (○) for LSD and HSD (*A*) and LSD and DOCA-salt diet (*B*). ****P* < 0.001, *****P* < 0.0001 compared to ANOVA followed by Sidak's multiple comparisons test.

a similar (Na$^+$+K$^+$) relative to water of ∼150 mmol L^{-1} (Fig. 6B) in myocardial tissue isolated from apex.

Na$^+$ concentration in skeletal muscle interstitial fluid and intracellular storage

Because of the observations above suggesting intracellular Na$^+$ storage, we therefore assessed Na$^+$ and K$^+$ in interstitial fluid isolated from hindlimb skeletal muscle. HSD did not result in significant changes in Na$^+$ and K$^+$ in muscle interstitial fluid (Fig. 7A), whereas the concentration of Na$^+$ increased during DOCA-salt ($n = 5$) diet averaging (mean ± SD) 154.0 ± 6.4 mmol L^{-1} H$_2$O significantly higher than the mean concentration in LSD ($n = 6$) of 142.2 ± 7.6 mmol L^{-1} H$_2$O ($P = 0.0222$) (Fig. 7A). This increase in Na$^+$ was accompanied by a decrease in K$^+$ compared to LSD (3.2 ± 0.7 mmol L^{-1} H$_2$O and 7.0 ± 1.1 mmol L^{-1} H$_2$O, respectively) ($P < 0.0001$) (Fig. 7A).

The assessed interstitial fluid and tissue concentration of Na$^+$, ECV, water content and thus ICV enable us to calculate the content of Na$^+$ contained in the ECV and ICV during variation of salt intake (Fig. 7B). By such calculations, we find that, although the interstitial content was moderately increased, HSD led to a modest and DOCA-salt to a dramatic intracellular passage of Na$^+$ resulting in a concentration that was ∼8 times higher than the corresponding concentration in LSD.
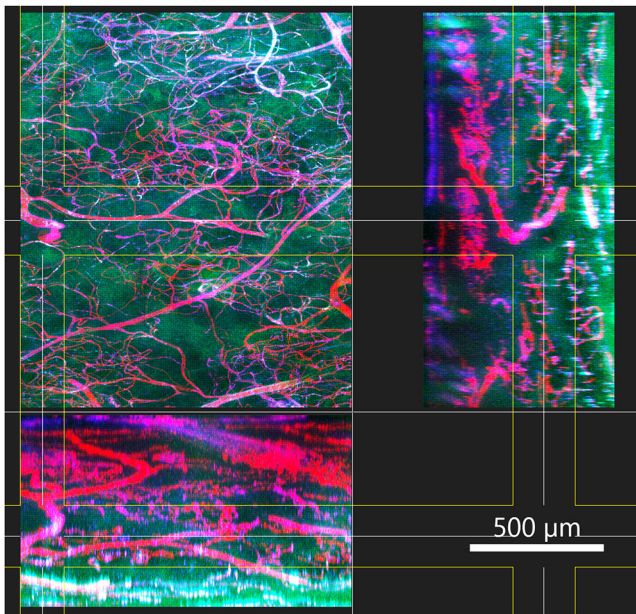

Figure 5. Two-photon image of skin
A rat was perfused with tomato lectin conjugated to DyLight® 649. Skin was collected and processed as described in the Methods. Blue, second harmonic generation (SHG); green, autofluorescence; red, lectin.

By applying the same interstitial fluid concentrations of Na$^+$ and K$^+$, we found that both high salt diets also resulted in intracellular accumulation of Na$^+$ in cardiac muscle (Fig. 7C), even though less pronounced than in skeletal muscle.

Discussion

In the present study, we addressed the question of Na$^+$ storage in skin that has recently been proposed to have an essential role in fluid homeostasis and to serve as a depot for Na$^+$ in several pathological conditions. We applied ion chromatography for high resolution element analysis combined with local extracellular fluid volume determination in tangential sections of rat skin and found that there might exist an interstitial fluid gradient in Na$^+$ between epidermis and dermis during low hydration, supporting the hypothesis of local microenvironmental electrolyte control. This notwithstanding, our study does not support a role of negatively charged sulphated glycosaminoglycans (sGAGs) proposed to bind and thus make Na$^+$ osmotically inactive and thereby serve as a buffer mechanism during high salt conditions. We found, however, evidence for intracellular storage of Na$^+$ without concomitant increase in hydration in dermis, as well as skeletal and cardiac muscle. Considering that skeletal muscle is the largest tissue in the rat, amounting to 45.5% of the rat weight (Caster et al., 1956), and that ∼65% of this is intracellular fluid, it follows that skeletal muscle can serve as a major Na$^+$ reservoir in situations of high salt intake.

Our main goal was to test the hypothesis that there is a gradient in Na$^+$ in skin such that there is an increasing concentration closer to the surface and that this gradient is consequence of a counter-current effect used for electrolyte gradient formation in the kidney medulla. We addressed this question by two approaches: increasing the resolution of our previous electrolyte analysis of skin after dry ashing to ion chromatography after tissue elution and by two-photon imaging of skin vasculature. The ion chromatography approach gave results for whole skin Na$^+$ and K$^+$ in low and high salt conditions similar to those for the dry ashing that might be considered as a reference method. In addition, together with techniques to measure local extra- and intracellular volumes, the ion chromatography could technique inform about the local microenvironment in skin. We chose a thickness of 40 μm for the superficial layer to limit potential artefacts related to evaporation for all groups, even though the DOCA-salt group had a thinner epidermis than the LSD and HSD groups. Moreover, 40 μm also turned out to be a lower limit for sample size in tracer measurements of extracellular volume. The consequence of a thinner epidermis would

mean that the most superficial skin section in DOCA-salt also contained some dermis that, based on our results, would have tended to raise the content of Na^+ in this section. The pattern of ion distribution and the content was similar for the superficial layers in DOCA-salt and its respective LSD control group, suggesting that this thinning of epidermis did not influence the results. We acknowledge that our ion chromatography method has lower resolution regarding detecting gradients in ion content than electron probe microanalysis. Such analysis allows for local water assessment (Warner et al., 1988), but, up to now, not for differentiation between extra- and intracellular localization of the ions and thus the information sought in the present study.

In agreement with previous data (Karlsen et al., 2018; Nikpey et al., 2017), high salt diets caused a slight increase in skin water content, and a higher Na^+ concentration expressed per gram dry weight, as well as water. Interestingly, a high salt diet led to a selective ion accumulation in dermis shown by an increase of $\sim$20 mmol L^{-1} H_2O in $(Na^+ + K^+)$ in the HSD and DOCA-salt group relative to LSD. The stored Na^+ may accumulate in the extra- as well as the intracellular phase, whereas the present data point to the intracellular fluid phase as

the predominant for storage in skin. This assumption is based on our finding of no increase in skin interstitial fluid Na^+ either isolated from wicks or as lymph that comprises a surrogate for interstitial fluid (Nikpey et al., 2017). It might be argued that an increased mass of Na^+ can be bound to or inactivated by GAGs (Schafflhuber et al., 2007), but the unaltered or actually lower sGAGs having capacity for Na^+ binding (see below) counters this option.

Glycosaminoglycans, that have a net negative charge, and in particular sulphated moieties (sGAGs), have been proposed to have a central role in Na^+ homeostasis originating from their ability to bind Na^+, thereby making Na^+ osmotically inactive, thus serving as a Na^+ reservoir (Schafflhuber et al., 2007; Titze et al., 2004). This proposal is based on findings of an increased fraction of sulphated relative to un-sulphated GAGs, namely hyaluronan, in skin of rats given 8% NaCl for 4 weeks (Schafflhuber et al., 2007). The relative increase in sGAGs was shown in titration experiments to result in an increased charge density in high salt conditions and an increase in Na^+ binding capacity and thereby the capacity to make Na^+ osmotically inactive. An increase in total GAGs and a relative increase in sGAGs was also found in patients with
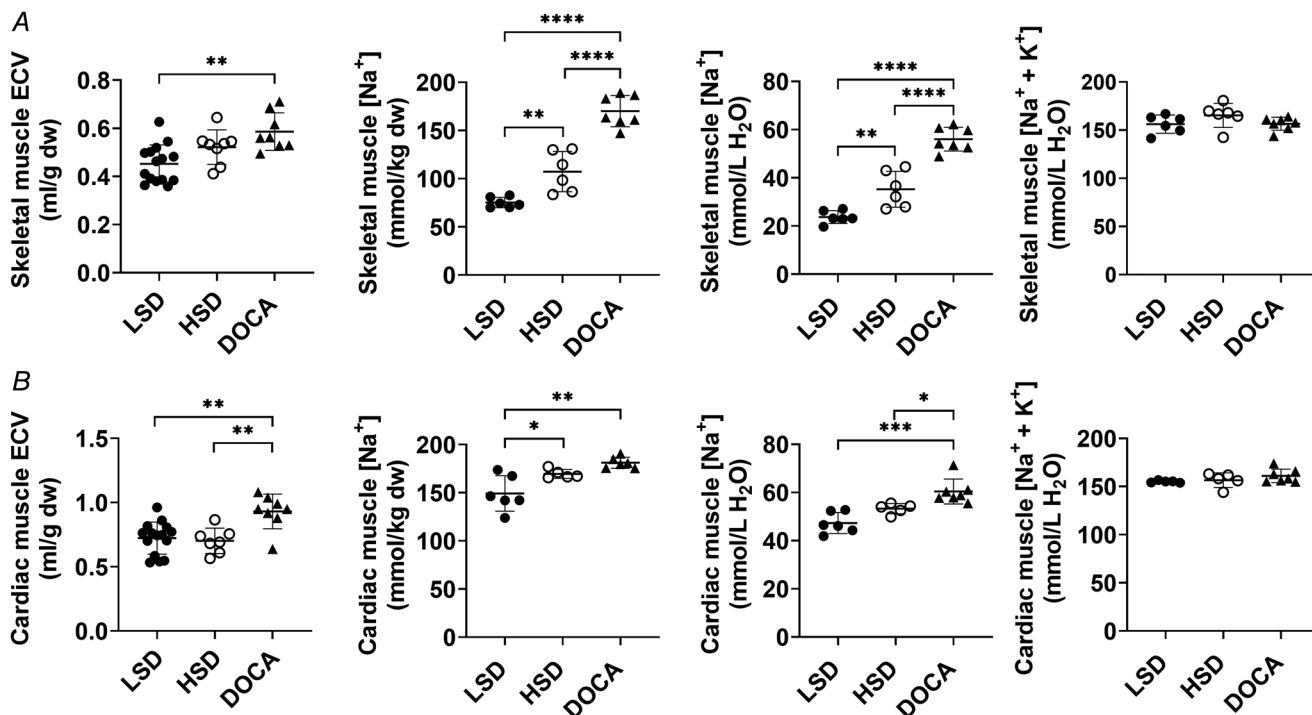

Figure 6. Na^+ and K^+ concentrations in skeletal and cardiac muscle
Extracellular fluid content per wet weight (WW), Na^+ concentration related to dry weight (DW) and water, and $Na^+ + K^+$ related to water in skeletal muscle (*A*) (left: LSD, $n = 15$; HSD, $n = 8$; DOCA, $n = 7$; middle and right: LSD, $n = 6$; HSD, $n = 6$; DOCA, $n = 7$) and cardiac muscle (*B*) (left: LSD, $n = 15$; HSD, $n = 8$; DOCA, $n = 7$; middle and right: LSD, $n = 6$; HSD, $n = 5$; DOCA, $n = 7$) in low salt diet (LSD) (●), high salt diet (HSD) (○), and deoxycorticosterone (DOCA)-salt diet (DOCA) (▲). Individual values and the mean ± SD are shown. *$P < 0.05$, **$P < 0.01$, ***$P < 0.001$, ****$P < 0.0001$ compared to ANOVA followed by Sidak's multiple comparisons test.

heart failure with increased tissue water content and peripheral (extracellular) oedema and thus tissue Na$^+$ content (Nijst et al., 2018). Other studies have shown that the amount of GAGs with Na$^+$-binding capacity correlates positively with skin Na$^+$ content in humans (Fischereder et al., 2017), as well as rats (Kopp et al., 2018; Sugar et al., 2018), all suggesting an active role for GAGs in Na$^+$ storage. We have no explanation for our finding that sGAGs were unaffected by salt load. Methodological issues may be involved because we applied a colorimetric assay, whereas, in previous studies, HPLC-based methods have been used. Our observation of significant salt storage as in previous studies despite no increase in sGAGs may indicate that the importance of sGAGs in salt storage is of less quantitative importance than suggested in the above referred studies.

Recent data, however, support our conclusion that GAGs are uncoupled from Na$^+$ storage. In HSD rats, Agocs et al. (2020) investigated salt accumulation and the effect of cyclooxygenase 2 (COX-2) inhibition. In line with previous reports, it was found that HSD not only resulted in increased chondroitin sulphate, namely an sGAG, but also un-sulphated hyaluronan. Interestingly, upon COX-2/prostaglandin E2 inhibition in HSD, the rats still retained salt to the same level as vehicle treated HSD rats, whereas their non- and sulphated GAGs returned to the control level as represented by LSD rats. In an attempt to resolve apparently conflicting data on GAGs in relation to salt storage and salt as a stimulus for GAG synthesis, we have previously suggested that inflammation and mechanical stress are inducers of GAG synthesis common to previous studies, and that Na$^+$ accumulation *per se* is not the inducer of GAGs (Wiig, 2018). Na$^+$ accumulates when GAGs are reduced by anti-inflammatory treatment, suggesting that agents other than Na$^+$ are a stimulus for its synthesis. Apparently, additional studies are needed to resolve these controversial data. Such studies should include an assessment of Cl$^-$ because osmotic inactivation of Na$^+$ by negatively charged GAGs relies on repulsion of Cl$^-$ (Farber et al., 1957), and Cl$^-$, in contrast to what might be expected from this inactivation, was increased rather than reduced in rat skin in our previous study (Wiig et al., 2013).

A central question in the present study was whether there was a concentration gradient of Na$^+$ increasing from deeper layers of skin towards epidermis by a kind of counter-current amplification (Hofmeister et al., 2015), which was suggested to be made possible by vascular loops in human papillary dermis (Short, 1974) by the same mechanism as that of the renal medulla. Our two-photon microscopical analysis of rat back skin structure suggests that there are no superficial vascular loops in rat dermis and thus counter-current amplification does not take place in this organ. Our data showed that Na$^+$ content was low in epidermis, increased abruptly when entering dermis, and was even more from superficial to deeper dermis, a pattern that was amplified in high salt conditions. This is consistent with findings in human skin, where 7T ^{23}Na-magnetic resonance imaging has revealed that Na$^+$ accumulates in dermis opposite to subcutis (Linz et al., 2015). A counter-current mechanism, however, is not required for concentrating Na$^+$ in skin, which can be achieved by regulation of blood flow and water loss from the surface.
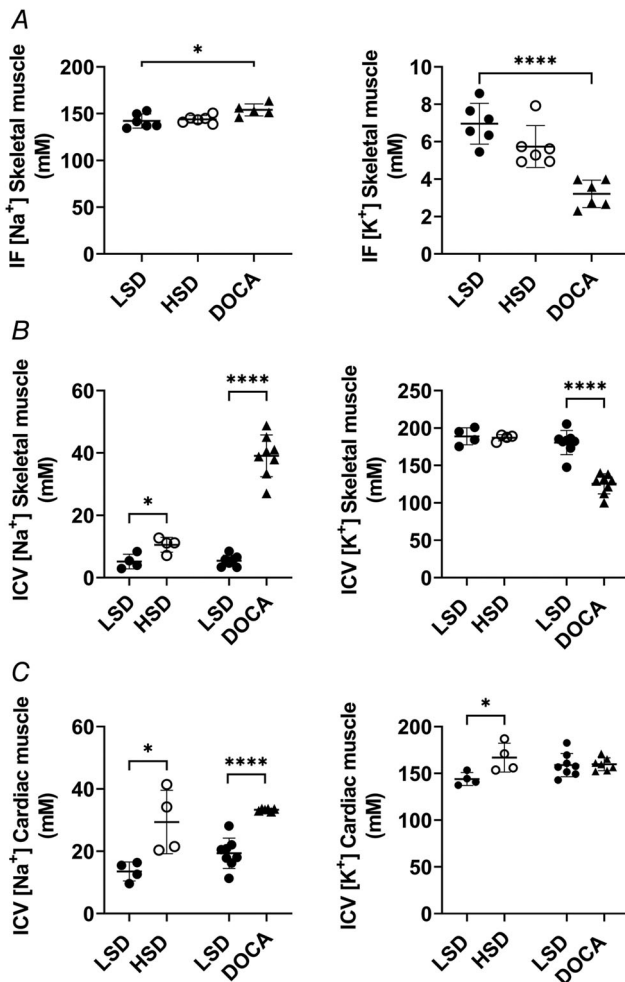

Figure 7. Na$^+$ and K$^+$ concentrations in skeletal muscle interstitial fluid and in skeletal and cardiac muscle intracellular volume

Na$^+$ (LSD, $n = 6$; HSD, $n = 6$; DOCA, $n = 5$) and K$^+$ (LSD, $n = 6$; HSD, $n = 6$; DOCA, $n = 6$) concentrations in interstitial fluid (IF) (*A*), in intracellular fluid volume (ICV) in skeletal muscle (*B*) and in ICV in cardiac muscle (*C*), in low salt diet (LSD) (●) (*n* = 4 in LSD and HSD series, *n* = 8 in LSD and DOCA series [except (*B*, left) where *n* = 7]), high salt diet (HSD) (○) (*n* = 4), and deoxycorticosterone (DOCA)-salt diet (DOCA) (▲) [*n* = 8 in (*B*), *n* = 6 in (*C*, left), *n* = 7 in (*C*, right)]. For the ICV calculations, the measured mean values of Na$^+$ and K$^+$ in IF in skeletal muscle were used. Individual values and the mean ± SD are shown. *$P < 0.05$ and ****$P < 0.0001$ compared to ANOVA followed by Sidak's multiple comparisons test.

We found no selective accumulation of Na^+ in superficial dermis and epidermis as proposed previously (Hofmeister et al., 2015), but rather that Na^+ accumulated in deeper dermis in situations with excess intake. In later studies, an alternative role for the skin in fluid volume and blood pressure regulation was proposed, namely that of reducing water loss in situations jointly named as 'estivation' requiring water conservation. During high salt intake (Kitada et al., 2017), experimentally induced psoriasis resulted in skin evaporation and water loss (Wild et al., 2021) and, in a model of experimental chronic kidney failure involving insufficient concentration ability (Kovarik et al., 2021), it was found that water was conserved by osmolytes, notably urea, which was produced by muscle catabolism. Additionally, water was conserved by reduction of evaporation by skin vessel vasoconstriction that will increase vascular resistance and thus blood pressure. High salt intake results in catabolism and increased urea production is supported by our finding of increased urea gradient between epidermis and dermis in HSD (Nikpey et al., 2017). Na^+ and K^+ and their corresponding anions are, however, the major determinants of skin osmolality, and the role of urea in limiting skin evaporation is therefore uncertain.

Our study indicates, however, that a variation in extracellular space in epidermis affecting extracellular Na^+ concentration may contribute to water conservation. The HSD and DOCA-salt experiments with their corresponding LSD controls were run in two series separated in time. The series were comparable with respect to distribution volumes and water content except for epidermis, where tissue water content and ECV in HSD were about twice of that in the DOCA-salt series and paralleled by their respective LSD controls. This variation was unintentional and surprising. The environmental conditions in our AAALAC accredited animal facility were not different in the two situations and the hydration difference may reflect passive evaporation or active regulation of fluid loss through evaporation (Wild et al., 2021) and, moreover, may explain our finding of variable fluid spaces in numerous series of animal experiments over the years. The existence of osmolyte gradients is supported by our finding of increased osmolality in the upper 0.5 mm of skin during HSD (Wiig et al., 2013) and DOCA-salt (Nikpey et al., 2017). Such gradients will contribute to reduce evaporation, and an intracellular shift of water will up-concentrate Na^+ in the extracellular space, as can be calculated from our data, that will reduce evaporation.

Our findings of unaltered (HSD) or reduced (DOCA-salt) sulphated GAGs do not support the idea that GAGs are actively regulated, thus having a role for GAGs in salt and water homeostasis capable of making Na^+ 'inactive' (Titze et al., 2003, 2006). This notwithstanding, skeletal muscle and (assuming similar interstitial fluid Na^+ concentrations) myocardium appear to have different mechanisms than skin (i.e. dermis) for handling Na^+ excess. In these muscle tissues, HSD, and in particular DOCA-salt, as a result of the stimulation of the mineralocorticoid receptors (Jia et al., 2021), leads to a substantial increase in intracellular Na^+, which was exchanged by K^+ such that $(Na^+ + K^+)$ remained $\sim$150 mmol L^{-1} with unaltered tissue hydration. Such Na^+/K^+ exchange in skeletal muscle is in line with previous data (Titze et al., 2005, 2006; Ziomber et al., 2008). In dermis, however, HSD and DOCA-salt both resulted in an increase in Na^+ of $\sim$20 mmol L^{-1} that was not followed by an exchange of K^+ such that $Na^+ + K^+$ rose from $\sim$140 to $\sim$160 mmol L^{-1} for both high salt interventions with no or modest increases in water content. Even though this variation is assumed to be in the physiological range (Rossitto et al., 2020), if not inactivated, this may still represent a significant osmotic force of $\sim$40 mosmol kg^{-1} [$2\times (Na^+ + K^+)$] that may mobilise fluid to the tissue. Interestingly, we have found that high salt results in $\sim$20 mosmol kg^{-1} increase in osmolality in dermis (Nikpey et al., 2017; Wiig et al., 2013) in HSD, as well as DOCA-salt, associated with a modest or no increase in skin water content. Apparently, skeletal muscle and heart can act as osmotically neutral Na^+/K^+ exchangers, whereas, in skin, a part of the osmotic effect is 'inactivated' in agreement with previous data (Titze et al., 2006). The molecular mechanisms explaining tissue differences in Na^+ storage and for the observed osmotically neutral Na^+/K^+ exchange is unclear. That the myocardium can store Na^+ has been established by ^{23}Na-MRI in patients with Conn's syndrome (Christa et al., 2019). As discussed for skin, our data do not support a role of GAGs in Na^+ inactivation as suggested by others (Schafflhuber et al., 2007). Evidently, Na^+ is stored intracellularly in situations of salt stress and may be osmotically inactivated by tissue specific negatively charged substances such as proteins present in the intracellular phase.

Considering our previous finding of an unaltered Na^+ concentration in lymph and thereby interstitial fluid (Nikpey et al., 2017), the observation of a marked increase in interstitial fluid Na^+ concentration in skeletal muscle in DOCA-salt rats was surprising. The upregulation of mineralocorticoid receptors by DOCA-salt (Jia et al., 2021) led to a dramatic increase in intracellular Na^+ that was shifted with K^+ and thus reduced intracellular K^+. Although at a lower scale, these shifts were paralleled in the interstitial fluid, suggesting that mineralocorticoid receptors also control the concentration of Na^+ and K^+ locally in this fluid phase in skeletal muscle and probably also in cardiac muscle. Whether these major shifts in Na^+/K^+ affect the electromechanical properties of myocardium and skeletal muscle remains to be

investigated in future studies. Interestingly, as reviewed in Pogwizd et al. (2003), heart failure and hypertrophy both lead to increased intracellular Na$^+$ that affects Ca^{2+} handling through the effect on Na/Ca exchange that can contribute to diastolic and/or systolic dysfunction and arrythmias, suggesting that high salt hypertension models also have a cardiac phenotype.

Clearly, the present study has limitations. We acknowledge that these ion shifts make our prediction of a high Na$^+$ concentration in the interstitial fluid of epidermis uncertain. Moreover, the high salt diet regimens probably induced a catabolic state that affected the tissue dry weight (Kitada et al., 2017) and handling of the tangential skin sections represents a challenge that may affect the numerical values reported. Although the present rat models of 8% salt in the diet and DOCA-salt both combined with 1% saline to drink are established for salt sensitive hypertension, they both represent an extreme salt load that may have questionable translational value. We used rats with hyperosmotic skin (Nikpey et al., 2017) to investigate whether osmotic gradients existed therein and whether there was a vessel structure that would enable salt gradients by a counter-current mechanism (Hofmeister et al., 2015). Although we found no support in the superficial skin vessel structure that would enable such a mechanism, we acknowledge that this might be different in humans. On the other hand, a specific structure is not a prerequisite for concentration gradients, which can be achieved by regulating the skin vascular resistance and loss of water from epidermis.

Perspectives

In the present study, we have found that there is no increase in Na$^+$ content in the superficial layers of rat skin. This notwithstanding, our data suggest that there is a hydration-dependent high interstitial fluid Na$^+$ concentration that will contribute to the skin barrier and thus be a mechanism for limiting the water loss shown to be a problem in skin diseases (Wild et al., 2021). An increase in GAGs, notably sulphated GAGs, has been found in several studies involving high salt intake or storage in rats, as well as humans, whereas we could not confirm an association between salt stress and GAG content. Our data do therefore not support a role of GAGs making Na$^+$ inactive in an osmotic sense. It appears that Na$^+$ is stored differently in skin and skeletal muscle and myocardium, and that Na$^+$ is inactivated in dermis by another mechanism, possibly intracellular proteins. Notably, the mechanism behind the major shifts in Na$^+$ and K$^+$ in skeletal muscle and myocardium, comprising shifts that may have electromechanical

consequences for contractile tissue, should be explored further.

References

Agocs, R., Pap, D., Sugar, D., Toth, G., Turiak, L., Vereb, Z., Kemeny, L., Tulassay, T., Vannay, A., & Szabo, A. J. (2020). Cyclooxygenase-2 modulates glycosaminoglycan production in the skin during salt overload. *Frontiers in Physiology*, **11**, 561722.

Caster, W. O., Poncelet, J., Simon, A. B., & Armstrong, W. D. (1956). Tissue weights of the rat. I. Normal values determined by dissection and chemical methods. *Proceedings of the Society for Experimental Biology and Medicine*, **91**, 122–126.

Christa, M., Weng, A. M., Geier, B., Wormann, C., Scheffler, A., Lehmann, L., Oberberger, J., Kraus, B. J., Hahner, S., Stork, S., Klink, T., Bauer, W. R., Hammer, F., & Kostler, H. (2019). Increased myocardial sodium signal intensity in Conn's syndrome detected by 23Na magnetic resonance imaging. *European Heart Journal Cardiovascular Imaging*, **20**, 263–270.

Farber, S. J., Schubert, M., & Schuster, N. (1957). The binding of cations by chondroitin sulfate. *Journal of Clinical Investigation*, **36**, 1715–1722.

Fischereder, M., Michalke, B., Schmockel, E., Habicht, A., Kunisch, R., Pavelic, I., Szabados, B., Schonermarck, U., Nelson, P. J., & Stangl, M. (2017). Sodium storage in human tissues is mediated by glycosaminoglycan expression. *American Journal of Physiology Renal Physiology*, **313**, F319–F325.

Guyton, A. C., Coleman, T. G., Cowley, A. W., Manning, R. D., Norman, R. A., & Ferguson, J. D. (1974). A systems analysis approach to understanding long-range arterial blood pressure control and hypertension. *Circulation Research*, **35**, 159–176.

Hall, J. E. (2016). Transport of substances through cell membranes. *Guyton and hall textbook of medical physiology* (pp. 47–59). Elsevier.

Heer, M., Baisch, F., Kropp, J., Gerzer, R., & Drummer, C. (2000). High dietary sodium chloride consumption may not induce body fluid retention in humans. *American Journal of Physiology Renal Physiology*, **278**, F585–F595.

Hofmeister, L. H., Perisic, S., & Titze, J. (2015). Tissue sodium storage: Evidence for kidney-like extrarenal countercurrent systems? *Pflugers Archiv: European Journal of Physiology*, **467**, 551–558.

Jia, G., Lockette, W., & Sowers, J. R. (2021). Mineralocorticoid receptors in the pathogenesis of insulin resistance and related disorders: From basic studies to clinical disease. *American Journal of Physiology Regulatory, Integrative and Comparative Physiology*, **320**, R276–R286.

Karlsen, T. V., Nikpey, E., Han, J., Reikvam, T., Rakova, N., Castorena-Gonzalez, J. A., Davis, M. J., Titze, J. M., Tenstad, O., & Wiig, H. (2018). High-salt diet causes expansion of the lymphatic network and increased lymph flow in skin and muscle of rats. *Arteriosclerosis, Thrombosis, and Vascular Biology*, **38**, 2054–2064.

Kitada, K., Daub, S., Zhang, Y., Klein, J. D., Nakano, D., Pedchenko, T., Lantier, L., LaRocque, L. M., Marton, A., Neubert, P., Schroder, A., Rakova, N., Jantsch, J., Dikalova, A. E., Dikalov, S. I., Harrison, D. G., Muller, D. N., Nishiyama, A., Rauh, M., … Titze J. (2017). High salt intake reprioritizes osmolyte and energy metabolism for body fluid conservation. *Journal of Clinical Investigation*, **127**, 1944–1959.

Kopp, C., Linz, P., Maier, C., Wabel, P., Hammon, M., Nagel, A. M., Rosenhauer, D., Horn, S., Uder, M., Luft, F. C., Titze, J., & Dahlmann, A. (2018). Elevated tissue sodium deposition in patients with type 2 diabetes on hemodialysis detected by (23)Na magnetic resonance imaging. *Kidney International*, **93**, 1191–1197.

Kovarik, J. J., Morisawa, N., Wild, J., Marton, A., Takase-Minegishi, K., Minegishi, S., Daub, S., Sands, J. M., Klein, J. D., Bailey, J. L., Kovalik, J. P., Rauh, M., Karbach, S., Hilgers, K. F., Luft, F., Nishiyama, A., Nakano, D., Kitada, K., & Titze, J. (2021). Adaptive physiological water conservation explains hypertension and muscle catabolism in experimental chronic renal failure. *Acta Physiologica (Oxford, England)*, **232**, e13629.

Linz, P., Santoro, D., Renz, W., Rieger, J., Ruehle, A., Ruff, J., Deimling, M., Rakova, N., Muller, D. N., Luft, F. C., Titze, J., & Niendorf, T. (2015). Skin sodium measured with (2)(3)Na MRI at 7.0 T. *NMR in Biomedicine*, **28**, 54–62.

Machnik, A., Neuhofer, W., Jantsch, J., Dahlmann, A., Tammela, T., Machura, K., Park, J. K., Beck, F. X., Muller, D. N., Derer, W., Goss, J., Ziomber, A., Dietsch, P., Wagner, H., van Rooijen, N., Kurtz, A., Hilgers, K. F., Alitalo, K., Eckardt, K. U., … Titze, J. (2009). Macrophages regulate salt-dependent volume and blood pressure by a vascular endothelial growth factor-C-dependent buffering mechanism. *Nature Medicine*, **15**, 545–552.

Nijst, P., Olinevich, M., Hilkens, P., Martens, P., Dupont, M., Tang, W. W. H., Lambrichts, I., Noben, J. P., & Mullens, W. (2018). Dermal interstitial alterations in patients with heart failure and reduced ejection fraction: A potential contributor to fluid accumulation? *Circulation Heart Failure*, **11**, e004763.

Nikpey, E., Karlsen, T. V., Rakova, N., Titze, J. M., Tenstad, O., & Wiig, H. (2017). High-salt diet causes osmotic gradients and hyperosmolality in skin without affecting interstitial fluid and lymph. *Hypertension*, **69**, 660–668.

Palacios, C., Wigertz, K., Martin, B. R., Jackman, L., Pratt, J. H., Peacock, M., McCabe, G., & Weaver, C. M. (2004). Sodium retention in black and white female adolescents in response to salt intake. *Journal of Clinical Endocrinology and Metabolism*, **89**, 1858–1863.

Pogwizd, S. M., Sipido, K. R., Verdonck, F., & Bers, D. M. (2003). Intracellular Na in animal models of hypertrophy and heart failure: Contractile function and arrhythmogenesis. *Cardiovascular Research*, **57**, 887–896.

Rakova, N., Juttner, K., Dahlmann, A., Schroder, A., Linz, P., Kopp, C., Rauh, M., Goller, U., Beck, L., Agureev, A., Vassilieva, G., Lenkova, L., Johannes, B., Wabel, P., Moissl, U., Vienken, J., Gerzer, R., Eckardt, K. U., Muller, D. N., … Titze, J. (2013). Long-term space flight simulation reveals infradian rhythmicity in human Na(+) balance. *Cell Metabolism*, **17**, 125–131.

Reed, R. K., Lepsoe, S., & Wiig, H. (1989). Interstitial exclusion of albumin in rat dermis and subcutis in over- and dehydration. *American Journal of Physiology*, **257**, H1819–H1827.

Rossitto, G., Mary, S., Chen, J. Y., Boder, P., Chew, K. S., Neves, K. B., Alves, R. L., Montezano, A. C., Welsh, P., Petrie, M. C., Graham, D., Touyz, R. M., & Delles, C. (2020). Tissue sodium excess is not hypertonic and reflects extracellular volume expansion. *Nature Communication*, **11**, 4222.

Sagstad, S. J., Oveland, E., Karlsen, T. V., Haslene-Hox, H., Tenstad, O., & Wiig, H. (2015). Age-related changes in rat dermal extracellular matrix composition affect the distribution of plasma proteins as a function of size and charge. *American Journal of Physiology Heart and Circulatory Physiology*, **308**, H29–H38.

Schafflhuber, M., Volpi, N., Dahlmann, A., Hilgers, K. F., Maccari, F., Dietsch, P., Wagner, H., Luft, F. C., Eckardt, K. U., & Titze, J. (2007). Mobilization of osmotically inactive Na$^+$ by growth and by dietary salt restriction in rats. *American Journal of Physiology Renal Physiology*, **292**, F1490–F1500.

Short, J. M. (1974). Disease of the blood vessels. In J. S. Dennis, R. L. Dobson, & J. McGuire (Eds.), *Clinical dermatology*, (pp. 1–9). Harper & Row.

Sugar, D., Agocs, R., Tatar, E., Toth, G., Horvath, P., Sulyok, E., & Szabo, A. J. (2018). The contribution of skin glycosaminoglycans to the regulation of sodium homeostasis in rats. *Physiological Research*, **67**, 777–785.

Titze, J., Bauer, K., Schafflhuber, M., Dietsch, P., Lang, R., Schwind, K. H., Luft, F. C., Eckardt, K. U., & Hilgers, K. F. (2005). Internal sodium balance in DOCA-salt rats: a body composition study. *American Journal of Physiology Renal Physiology*, **289**, F793–F802.

Titze, J., Lang, R., Ilies, C., Schwind, K. H., Kirsch, K. A., Dietsch, P., Luft, F. C., & Hilgers, K. F. (2003). Osmotically inactive skin Na+ storage in rats. *American Journal of Physiology Renal Physiology*, **285**, F1108–F1117.

Titze, J., Luft, F. C., Bauer, K., Dietsch, P., Lang, R., Veelken, R., Wagner, H., Eckardt, K. U., & Hilgers, K. F. (2006). Extrarenal Na+ balance, volume, and blood pressure homeostasis in intact and ovariectomized deoxycorticosterone-acetate salt rats. *Hypertension*, **47**, 1101–1107.

Titze, J., Maillet, A., Lang, R., Gunga, H. C., Johannes, B., Gauquelin-Koch, G., Kihm, E., Larina, I., Gharib, C., & Kirsch, K. A. (2002). Long-term sodium balance in humans in a terrestrial space station simulation study. *American Journal of Kidney Diseases*, **40**, 508–516.

Titze, J., Shakibaei, M., Schafflhuber, M., Schulze-Tanzil, G., Porst, M., Schwind, K. H., Dietsch, P., & Hilgers, K. F. (2004). Glycosaminoglycan polymerization may enable osmotically inactive Na+ storage in the skin. *American Journal of Physiology Heart and Circulatory Physiology*, **287**, H203–H208.

Warner, R. R., Myers, M. C., & Taylor, D. A. (1988). Electron probe analysis of human skin: Element concentration profiles. *Journal of Investigative Dermatology*, **90**, 78–85.

Wei, X., Roomans, G. M., & Forslind, B. (1982). Elemental distribution in guinea-pig skin as revealed by X-ray micro-analysis in the scanning transmission microscope. *Journal of Investigative Dermatology*, **79**, 167–169.

Wiig, H. (2018). Regulation of fluid volume from the outside: A role of glycosaminoglycans in the skin interstitium? *Circulation Heart Failure*, **11**, e005135.

Wiig, H., Schroder, A., Neuhofer, W., Jantsch, J., Kopp, C., Karlsen, T. V., Boschmann, M., Goss, J., Bry, M., Rakova, N., Dahlmann, A., Brenner, S., Tenstad, O., Nurmi, H., Mervaala, E., Wagner, H., Beck, F. X., Muller, D. N., Kerjaschki, D., … Titze, J. (2013). Immune cells control skin lymphatic electrolyte homeostasis and blood pressure. *Journal of Clinical Investigation*, **123**, 2803–2815.

Wiig, H., Sibley, L., DeCarlo, M., & Renkin, E. M. (1991). Sampling interstitial fluid from rat skeletal muscles by intermuscular wicks. *American Journal of Physiology*, **261**, H155–H165.

Wild, J., Jung, R., Knopp, T., Efentakis, P., Benaki, D., Grill, A., Wegner, J., Molitor, M., Garlapati, V., Rakova, N., Marko, L., Marton, A., Mikros, E., Munzel, T., Kossmann, S., Rauh, M., Nakano, D., Kitada, K., Luft, F., … Karbach, S. (2021). Aestivation motifs explain hypertension and muscle mass loss in mice with psoriatic skin barrier defect. *Acta Physiologica (Oxford, England)*, **232**, e13628.

Woessner, J. F. (1961). The determination of hydroxyproline in tissue and protein samples containing small proportions of this imino acid. *Archives of Biochemistry and Biophysics*, **93**, 440–447.

Ziomber, A., Machnik, A., Dahlmann, A., Dietsch, P., Beck, F. X., Wagner, H., Hilgers, K. F., Luft, F. C., Eckardt, K. U., & Titze, J. (2008). Sodium-, potassium-, chloride-, and bicarbonate-related effects on blood pressure and electrolyte homeostasis in deoxycorticosterone acetate-treated rats. *American Journal of Physiology Renal Physiology*, **295**, F1752–F1763.

Additional information

Data availability statement

All data described in the present study are included in the main manuscript or the Supporting information.

Supporting information

Additional supporting information can be found online in the Supporting Information section at the end of the HTML view of the article. Supporting information files available:

Statistical Summary Document
Peer Review History
Supporting Video